Materials and Structures
DOI 10.1617/s11527-011-9715-z

ORIGINAL ARTICLE

Crack width for thick offshore plates

E. Rizk · H. Marzouk · A. Hussein

Received: 13 November 2009 / Accepted: 23 February 2011

Abstract Using thick concrete covers in offshore and nuclear containment applications is increasing because it is a durability issue. Most crack width models indicate that increasing concrete covers results in increased crack spacing and hence increased crack width this means that thick concrete covers are detrimental to crack control. In this paper, tests were conducted on two groups of thick plates. Group I, included five specimens that had two concrete covers, 60 and 70 mm. Group II, included four thick heavy reinforced specimens; all specimens in this group had a clear concrete cover of 70 mm. Using thick concrete covers is a common practice in offshore and containment structures for nuclear power generation. The objective of testing both groups is to measure flexural crack widths under different load levels and, most importantly, under service loads. Group I was intended primarily to investigate the effect of increasing the cover and bar spacing on the crack width. Group II represents a unique experimental investigation in assessing the magnitude of crack width in full-scale thick plates under service loads. An analytical investigation is presented in this work. The main focus of this study is to evaluate the available codes' models for estimating the crack width of thick concrete plates having thick concrete covers used for offshore and nuclear containment structure applications. It was concluded that crack control can still be achieved by limiting the spacing of the reinforcing steel despite using thick concrete covers.

Keywords Thick plates · Crack spacing · Crack width · Thick concrete covers · Bar spacing

Notations

$A_{c,\mathrm{ef}}$	Area of concrete symmetric with reinforcing steel divided by number of bars
A_s	Area of reinforcement within the effective embedment thickness
b	Width of the section
c	Concrete cover or the depth under compression
C_c	Clear cover from the nearest surface in tension to the flexural tension reinforcement
d	Effective depth to the centroid of the tensile reinforcement
d_b	Reinforcing bar diameter
d_c	Thickness of cover from the extreme tension fiber to the closest bar
E_c	Concrete modulus of elasticity
E_s	Steel modulus of elasticity
f_{bo}	Maximum bond strength

E. Rizk · A. Hussein
Faculty of Engineering and Applied Science, Memorial University of Newfoundland, St. John's, Newfoundland A1B 3X5, Canada

H. Marzouk (✉)
Department of Civil Engineering, Faculty of Engineering, Architecture and Science, Ryerson University, Toronto, ON M5B 2K3, Canada
e-mail: hmarzouk@ryerson.ca

Published online: 18 March 2011

f'_c	Uniaxial compressive strength of concrete (cylinder strength)
f_{ctm}	The mean value of the concrete tensile strength at the time that the crack forms
f_s	Stress in reinforcement due to applied load
f_y	Yield stress of steel
h	Section height
h_{ef}	Effective embedment thickness
k_t	Tensile stress factor
s	Center-to-center spacing of flexural tension reinforcement nearest to the surface of the extreme tension face
S_m	Average stabilized crack spacing
S_{mx}	The crack spacing for cracks normal to x reinforcement
S_{my}	The crack spacing for cracks normal to y reinforcement
$S_{r,\max}$	Maximum crack spacing
β	Coefficient relating the average crack width to the design value
ε_1	The largest tensile strain in the effective embedment zones
ε_2	The smallest tensile strain in the effective embedment zones
$\varepsilon_{\mathrm{cm}}$	The average strain in the solid concrete between the cracks
$\varepsilon_{\mathrm{sm}}$	The strain under relevant combination of loads and allowing for effects, such as tension stiffening or shrinkage

1 Introduction

This research is focused on evaluating the effect of using thick concrete covers up to 70 mm on crack widths and crack properties of thick plates up to 400 mm thickness used for offshore and nuclear containment structures. The crack width depends on the amount and distribution of reinforcing steel across the crack, concrete cover thickness and characteristics of the bond between the concrete and reinforcement bars in and near the crack. Using thick concrete covers for offshore and nuclear containment applications is increasing because it is a durability issue, and also thick concrete covers resist and delay steel reinforcement corrosion. Most crack width models indicate that increasing concrete covers results in increased crack spacing and hence increased crack width this means that thick concrete covers are detrimental to crack control. The current experimental study tries to assess the effect of thick covers on crack widths. Also, one of the objectives of this experimental investigation is to evaluate the accuracy of design codes' models when dealing with thick plates having thick concrete covers. Provisions based on limiting crack width need to be re-examined in light of the requirements for a durable concrete in aggressive environments.

Tests were conducted on two groups of thick plates. The first group is intended primarily to investigate the effect of increasing the cover, bar diameter and bar spacing on the crack width. Whereas the second group is intended to investigate the effect of increasing bar spacing on the crack width. The objective of testing both groups was to measure flexural crack widths under different load levels and, most importantly, under service loads.

The paper also, presents a crack width model that could be applied to thick concrete plates having thick concrete covers. The proposed model is based on a crack spacing model proposed by Rizk and Marzouk [1]. The crack width predictions have been shown to provide good agreement with the measured crack width in a variety of slabs and beams tested by different researchers.

2 Research significance

One of the objectives of this research is to evaluate the accuracy of design codes' models when dealing with thick plates having thick concrete covers. This paper presents a unique experimental investigation for large size slabs. Nine thick plates having thick concrete covers had been tested to examine the accuracy of available crack width models in different design codes. Analytical investigation is presented that aims to propose a simple and more accurate crack width model to help design engineers.

3 Previous research

The effect of thick concrete covers on the maximum flexural crack width was studied by Makhlouf and Malhas [2]. Two groups of rectangular beams were tested, the first group contained sixteen beam specimens having different reinforcement ratios and different concrete covers designed to investigate the effect of increased cover on crack width. The second group contained eight beam specimens; this testing group was intended to evaluate the magnitudes of surface crack widths under service load when using a 50 mm thick concrete cover. The researchers showed that the use of a 50 mm concrete cover leads to acceptable levels of crack widths under service loads. Another finding was, the increase in concrete cover to the main reinforcement from 30 to 60 mm leads to an increase in the measured crack width of 16%, compared to 80% increase in crack width as a result of increasing the concrete cover by the same amount calculated by both ACI 318-89 [3] and BS 8110-85 [4]. This means that thick concrete covers can be used to increase durability of offshore structures and at the same time crack control requirements are not violated.

As reported by Frosch [5], concrete covers only up to 65 mm have been used in experiments considered by Gergely and Lutz [6] in the development of the prediction formula. As a result, the applicability of ACI 318-95 [7] prediction procedure (that is based on Gegely and Lutz [6] formula) is questionable in cases where the concrete cover exceeds 65 mm.

Therefore, an alternative statistical approach for the calculation of crack widths based on available cracking data is proposed for thicker concrete covers ($d_c \geq 63$ mm) by Frosch [5]. The new approach assumes the crack width as a function of bar spacing and concrete cover. Therefore, crack control can be achieved by limiting the spacing of the reinforcing steel. The equation for the maximum crack width of uncoated reinforcement is:

$$w_c = 2\frac{f_s}{E_s}\beta\sqrt{d_c^2 + \left(\frac{s}{2}\right)^2} \tag{1}$$

where w_c is the limiting crack width, s is the maximum permissible bar spacing, d_c is the bottom cover measured from the center of the bar, f_s is the calculated stress in reinforcement at service load = unfactored moment divided by the product of steel area and internal moment arm. Alternatively at the serviceability limit, f_s can be taken as 0.6 f_y; and $\beta = 1.0 + 0.08\ d_c$.

Since the width of the crack at the surface of the tension side concrete is going to be wider than width of the crack at center of reinforcement level, β is used as an amplification factor to account for the change of the strain over the beam section.

$$\beta = \frac{\varepsilon_2}{\varepsilon_1} = \frac{h-c}{d-c} \tag{2}$$

where ε_1 is the strain at the level of steel reinforcement, ε_2 is the strain at the tension surface of the concrete section, c is the depth under compression, d is the effective depth and h is the section height.

Frosch et al. [8] tested ten one-way slabs, the ten bridge deck specimens were designed to represent a full scale cut section from a bridge deck. Each specimen was prismatic, with a rectangular cross section ($b = 914$ mm, $h = 203$ mm and a span $l = 2438$ mm). The primary variables evaluated in the study were the spacing of the reinforcement and the epoxy coating thickness. The parameters varied in the tests were the reinforcing bars type, the spacing between bars, s, and the sustained load level. Frosch et al. [8] found that; as the reinforcement spacing decreased, the spacing of primary cracks decreased and the number of primary cracks increased; and as the reinforcement spacing increased, there was a corresponding increase in crack width. The researchers did not address the effect of transverse reinforcement on crack behavior. The spacing of the transverse cracks in reinforced concrete members subjected to flexure or direct tension are affected primarily by the spacing of the transverse reinforcement steel parallel to the direction of the cracks.

Gilbert and Nejadi [9] studied the cracking caused by shrinkage in restrained reinforced concrete members both experimentally and analytically. A total of twelve simply-supported beams and one-way slabs were subjected to constant sustained service loads for a period of 400 days. Each specimen was prismatic, with a rectangular cross section ($b = 250$ mm and $h = 348$ mm for the six beams; and $b = 400$ mm and $h = 161$ mm for the six one-way slabs) and a span of 3500 mm, and was carefully monitored throughout the test to record the time-dependent deformation, together with the gradual development of cracking and the gradual increase in crack widths with time. The parameters varied in the tests were the shape of the section b/d, the number of reinforcing bars, the spacing between bars s, the clear concrete cover C_c, and the sustained load level. Experimental observations by Gilbert and Nejadi [9] indicate that, the bond stress reduces as the stress in the reinforcement increases and, consequently, the tensile stresses in the concrete between the cracks reduce (that is, tension stiffening reduces with increasing steel stress).

Hossin and Marzouk [10] tested eight square full scale specimens to investigate the crack width and spacing of high strength concrete slabs, five high strength concrete slabs (HSC) and three normal strength concrete slabs (NSC). The structural behaviour with regards to deformation and strength characteristic of high strength concrete slabs of various thicknesses and different reinforcement ratios (0.40–2.68%) were studied. The test results revealed that as the concrete cover increases by 67%, the average crack width becomes larger by 90% experimentally. While increasing the bar spacing by 67%, increases the crack width by 19%. However, increasing the bar spacing further does not affect the crack width.

4 Codes provisions for crack width calculations

4.1 ACI 318-08 [11] approach

A reevaluation of cracking data [5] provided a new equation based on the physical phenomenon for the determination of the flexural crack widths of reinforced concrete members. This study showed that previous crack width equations are valid for a relatively narrow range of covers (up to 63 mm). ACI 318-08 [11] does not make a distinction between interior and exterior exposure. It requires that for crack control in beams and one-way slabs, the spacing of reinforcement closest to a surface in tension shall not exceed that given by:

$$s = 380\left(\frac{280}{f_s}\right) - 2.5\,C_c \tag{3}$$

but not greater than 300 (280/f_s), where s is center-to-center spacing of flexural tension reinforcement nearest to the extreme tension face, f_s is calculated stress in reinforcement at service load computed as the unfactored moment divided by the product of steel area and internal moment arm. It is permitted to take f_s as 0.67 f_y, and C_c is clear cover from the nearest surface in tension to the surface of flexure tension reinforcement.

4.2 CSA-S474-04 [12] offshore code

The Canadian offshore code (CSA-S474-04) [12] recommends that the average crack width may be calculated as the average crack spacing times the total average tensile concrete strain after considering the contribution of the tension stiffening. Both NS 3473 E (1989) [13] and CSA-S474-04 [12] provide similar expressions for calculating crack spacing. CSA-S474-04 [12] estimates the crack width at the surface of the member. However, NS 3473 E (1989) [13] calculates the crack width at the level of steel reinforcement. CSA-S474-04 [12] provides the following expression for calculating the crack spacing:

$$S_m = 2.0(C_c + 0.1\,s) + k_1\,k_2\,d'_{\mathrm{be}}\,h_{\mathrm{ef}}\,b/A_s \tag{4}$$

where S_m is the average crack spacing, C_c is clear concrete cover, s is bar spacing of outer layer, k_1 is coefficient that characterizes bond properties of bars, $k_1 = 0.4$ for deformed bars, $k_1 = 0.8$ for plain bars, this is related to the deformed rips on bars; k_2 is coefficient to account for strain gradient; d'_{be} is bar diameter of outer layer, h_{ef} is effective embedment thickness (Fig. 1) as the greater of (C_c + d'_{be}) + 7.5d'_{be} and $a_2 + 7.5d'_{\mathrm{be}}$ but not greater than the tension zone or half slab thickness, b is width of the section and A_s is area of reinforcement within the effective embedment thickness.

4.3 Norwegian code

The contribution of concrete in tension between cracks in European codes is taken as a reduction factor of the total concrete strain. The Norwegian code, NS 3473E (1989) [13], provides the following equation for calculating the crack width. It uses factor r to account for tension stiffening effect.

$$w_k = 1.7\,w_m \tag{5}$$

$$w_m = r\,\varepsilon_1\,S_{\mathrm{rm}} \tag{6}$$

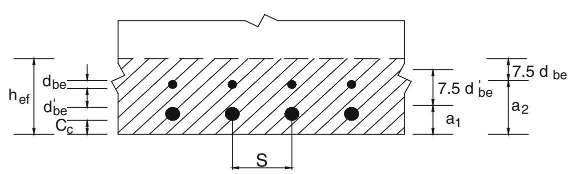

Fig. 1 Effective embedment thickness (effective tension area)

$$r = 1 - \frac{\beta}{2.5\,k_1}(\sigma_{sr}/\sigma_s)^2 \geq 0.4 \qquad (7)$$

where w_k is the characteristic maximum crack width, w_m is the average crack width, ε_1 is the principal tensile strain at level of tensile reinforcement, $\varepsilon_1 = \varepsilon_s = \sigma_s/E_{sk}$, σ_s is the stress in the reinforcement in the crack, σ_{sr} is the stress in the reinforcement at calculated crack, E_{sk} is the characteristic modulus of elasticity of steel, k_1 is a coefficient that characterizes bond properties of bars, β is a coefficient that accounts for type of action, and S_{rm} is the mean crack spacing. The NS 3473E (1989) [13] code calculates the maximum characteristic crack width w_k at the level of steel reinforcement. The characteristic crack width is defined in most of the European codes as the width that only 5% of the cracks will exceed. This characteristic crack width is taken as 70% more than the average crack width. The NS 3473E (1989) [13] code provides more detailed regulations for crack width limitations depending on the environmental conditions. Four environment classes are identified; namely, especially aggressive, severely aggressive, moderately aggressive and mildly aggressive environment.

4.4 CEB-FIP (1990) [14] code

The CEB-FIP (1990) [14] model code gives the following equation for calculation of the characteristic crack width:

$$w_k = l_{s,\max}\left(\varepsilon_{s2} - \beta\,\varepsilon_{sr2} - \varepsilon_{cs}\right) \qquad (8)$$

where $l_{s,\max}$ is the length over which slip between steel and concrete occurs, w_k is characteristic maximum crack width, w_m is average crack width, ε_{s2} is steel strain of transformed section in which the concrete in tension is ignored, ε_{cs} is the free shrinkage of concrete, generally a negative value, ε_{sr2} is the steel strain at crack, under a force causing stress equal to f_{ctm}, within A_{cef}. To account for tension stiffening in the CEB-FIP (1990) [14] code, an empirical shape factor β is used to assess the average strain within $l_{s,\max}$.

4.5 Eurocode EC2 (2004) [15] provisions

The characteristic crack width as given by EC2 (2004) [15] design code is estimated by the following expression as:

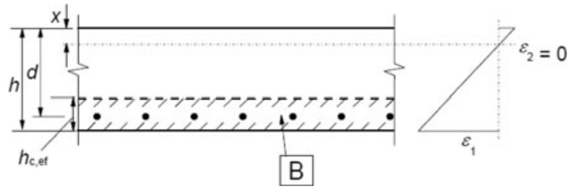

Fig. 2 Effective tension area (slab)

$$w_k = S_{r,\max}\left(\varepsilon_{sm} - \varepsilon_{cm}\right) \qquad (9)$$

where $S_{r,\max}$ is the maximum crack spacing, ε_{sm} is mean strain under relevant combination of loads and allowing for effects, such as tension stiffening or shrinkage, and ε_{cm} is the average strain in the solid concrete between the cracks. The maximum crack spacing, $S_{r,\max}$, is evaluated from the following expression:

$$S_{r,\max} = 3.4\,c + 0.425\,k_1\,k_2\frac{\phi}{\rho_{\text{eff}}} \qquad (10)$$

where c is concrete cover, mm, ρ_{eff} is effective reinforcement ratio $= A_s/A_{c,\text{eff}}$ (see Fig. 2), k_1 is coefficient that takes into account bar surface equals 0.8 for ribbed/deformed bars and 1.6 for smooth/plain bars, and k_2 is coefficient that takes into account strain gradient over the cross section equals 0.5 for bending and 1.0 for pure tension. The value of $(\varepsilon_{sm} - \varepsilon_{cm})$ is evaluated by EC2 (2004) [15] as follows:

$$\varepsilon_{sm} - \varepsilon_{cm} = \frac{\sigma_s - k_t\frac{f_{\text{ct,eff}}}{\rho_{p,\text{eff}}}\left(1 + \alpha_e\,\rho_{p,\text{eff}}\right)}{E_s} \geq 0.6\frac{\sigma_s}{E_s} \qquad (11)$$

where σ_s is the stress in steel, evaluated for the related combination of actions under the assumption of cracked cross section; $\alpha_e = E_s/E_c$; and $k_t = 0.6$ for short term loadings and 0.4 for long term loadings.

5 Experimental investigation

The variables considered in the current investigation are the concrete cover and bar spacing for normal and high strength concrete plates. The selected values for the proposed experimental testing are typical for the possible use in Canadian offshore applications (CSA-S474-04 [12]). The experimental investigation included testing of nine reinforced concrete thick plates in the structural lab at Memorial University of Newfoundland (MUN).

Six high strength concrete slabs (HS) and three normal strength concrete slabs (NS) were selected for the experimental investigation of the cracking behavior study as detailed in Table 1; details of a typical test specimen are shown in Fig. 3. The slabs thicknesses ranged from 250 to 400 mm and were designed to examine the effect of concrete cover and bar spacing on the cracking behavior.

The first group (Group I) was designed to investigate the effect of concrete cover, concrete strength and corresponding change in steel ratio for the same bar spacing on the crack width. Group I included five test specimens. The slabs of this group had different slab thicknesses, 250 and 300 mm, two thick concrete covers, and different bar size, 15, 20 and 25 M. All the slabs had the same big bar spacing of 368 mm. The first two slabs had 67.5 mm cover (60 mm clear cover), and the rest of slabs had 82.5 mm cover (70 mm clear cover).

The second group (Group II) contained four slabs designated as HS4, HS5, NS3 and HS6; all these slabs except slab HS4 had high reinforcement ratio and were designed to investigate the effect of bar spacing on the crack spacing and crack width. The slabs of this group had the same thick concrete cover 70 mm, but different bar diameters, 25 and 35 M, and different bar spacing of 217, 289 and 368 mm. The first two slabs had the same thickness (350 mm). The next two slabs had the same thickness (400 mm) and the same bar spacing with different concrete strengths.

All the specimens of the first group (Group I) were designed to fail under flexure failure as recommended by Marzouk and Hussein [16]. However, all the specimens of the second group (Group II) except specimen HS4 were designed to investigate the effect of other modes of failure on crack width. The specimens in this Group were designed to fail under punching failure mode.

Table 1 Details of test specimens

Group no.	Slab no.[a]	Compressive Strength f_c' (MPa)	Bar size (mm)	Bar spacing (mm)	Concrete cover C_c (mm)	Slab thickness (mm)	Depth (mm)	Steel ratio (ρ%)
I	NS1	35.0	15	368	60	250	182.5	0.35
	HS1	70.0	15	368	60	250	182.5	0.35
	NS2	35.0	25	368	70	300	217.5	0.73
	HS2	64.7	25	368	70	300	217.5	0.73
	HS3	70.0	20	368	70	300	220.0	0.43
II	HS4	76.0	25	368	70	350	267.5	0.50
	HS5	65.4	35	289	70	350	262.5	1.42
	NS3	40.0	35	217	70	400	312.5	1.58
	HS6	60.0	35	217	70	400	312.5	1.58

[a] *NS* normal strength slabs, *HS* high strength slabs

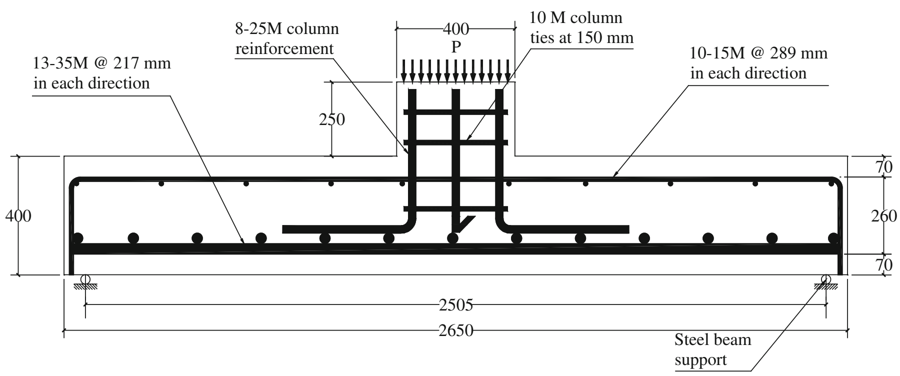

Fig. 3 Details of typical test specimen HS6 ($h = 400$ mm)

5.1 Crack width measurements

The test specimens were initially loaded up to 10% of the ultimate load. Then Crack Displacement Transducers (CDT) were mounted on the concrete surface of the first, second and third visible cracks on the tension surface of the slab in order to measure the crack opening displacement as shown in Fig. 4. The surface crack gauges were installed using epoxy glue and were left for 1 hour in order to enable the epoxy to dry before resuming the loading of the specimen. The load was released and then reapplied at a selected load increment of 44.0 kN (10 kips). The test slabs were carefully inspected at each load step. The cracks were marked manually after mapping all the cracks on the specimen. The crack displacement transducer is a waterproof enabled gauge. The range of the gauge is between ±2 to ±5 mm. The accuracy of the measurements improved as the cracks started to widen.

A large amount of test data was recorded and the related graphs were prepared. The behavior of the slabs was presented in terms of the load–deflection relationship at different load stages, including service and ultimate load, as well as steel strain–crack width relationships. Failure modes, crack patterns and crack spacing were also depicted by means of photographs. In this paper, our investigation will focus only on the data that relates to crack width and serviceability loading rather than ultimate loading and failure modes.

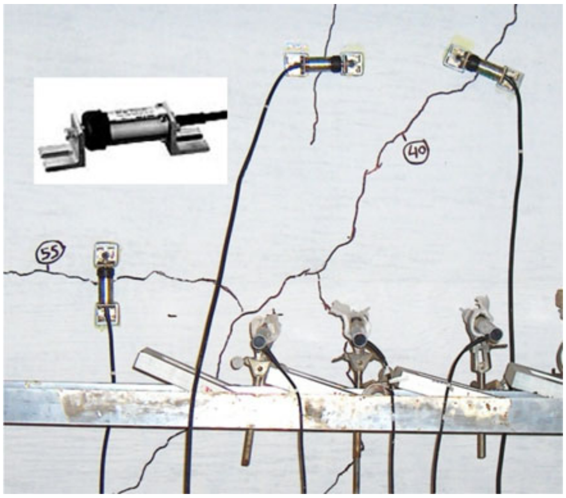

Fig. 4 Crack Displacement Transducers (KG-A)

5.2 Test results

5.2.1 Crack formation

The first crack in each specimen was visually inspected and the corresponding load was recorded as the first cracking load. The yield steel strain was assumed to occur at a value of 2000 $\mu\varepsilon$, which produced a stress in the steel rebar equal to 400 MPa. The yield strain was measured first at the center of the slab. In all test slabs, the initial observed cracks were first formed tangentially under the edge of the column stub, followed by radial cracking extending from the column edge toward the edge of the slab. As the load was increased, the tension reinforcement yielded, which resulted in a significant increase in the crack width and the deflection. Few slabs were failed under flexure mode and other slabs failed under punching shear mode.

For the slabs failing in flexure (NS1, HS1, HS3 and HS4), flexure yield lines were well developed. For the slabs failing by punching (NS2, HS2, NS3, HS5 and HS6), the first radial cracks were much more pronounced along the lines parallel to the reinforcement passing through the column stub. Orthogonal cracking was the most dominant crack pattern. As the load was increased, the tangential cracks were then extended outside the circumference of the stub column. Those tangential cracks were limited to the column vicinity. The slabs failed with the final shear crack coinciding with, or located outside, these tangential cracks. Final failure developed by the column punching through the slab. Failure pattern of typical test specimens is shown in Figs. 5 and 6.

5.2.2 Crack width

The crack width was measured at each load stage at different locations on the slab. In Figs. 7, 8, 9, 10, 11, 12, 13, 14, 15, the opening of the crack width is plotted versus the steel strain. It could be noticed that the crack width increased as the load and deflection were increased. It was noticed also, that the crack width versus steel strain can be represented by one straight line up to an average value of 2000 $\mu\varepsilon$ of steel strain.

The widths of the primary cracks were examined in the two sets of test specimens to determine the effect of bar spacing, bar diameter and concrete cover

Fig. 5 Crack pattern of test slab HS4 (radial crack pattern)

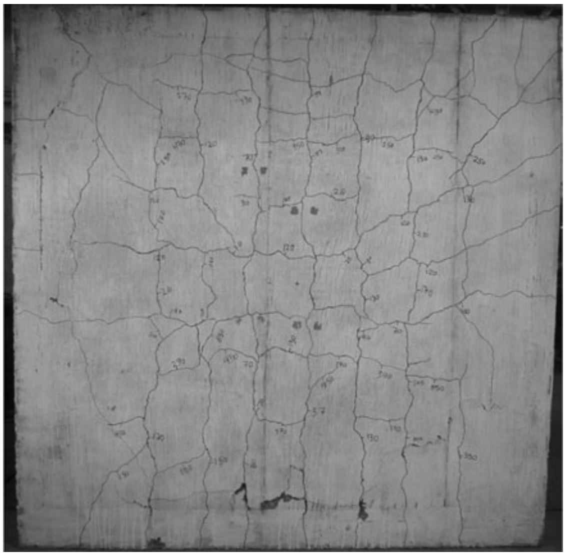

Fig. 6 Crack pattern of test slab HS5 (orthogonal crack pattern)

on the maximum crack width measurements. It was not possible to address the effect of change in slab thickness on the maximum crack width measurements when refereeing to data of group II, as the test specimens had different bar spacing.

All measurements reported in Table 2 were taken at a steel stress level of 267 MPa (0.67 f_y). The data showed that as the concrete cover was increased in Group I, the crack width increased. The maximum

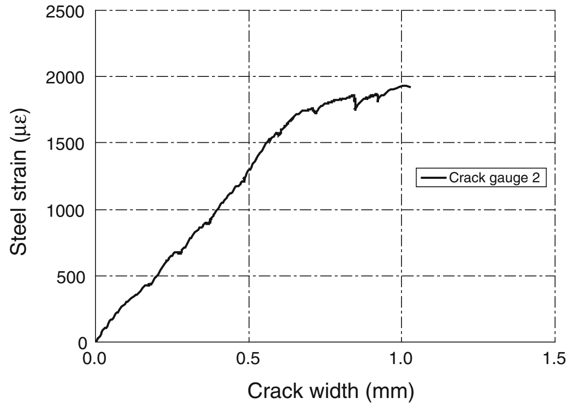

Fig. 7 Crack width expansion versus steel strain for NS1 ($h = 250$ mm)

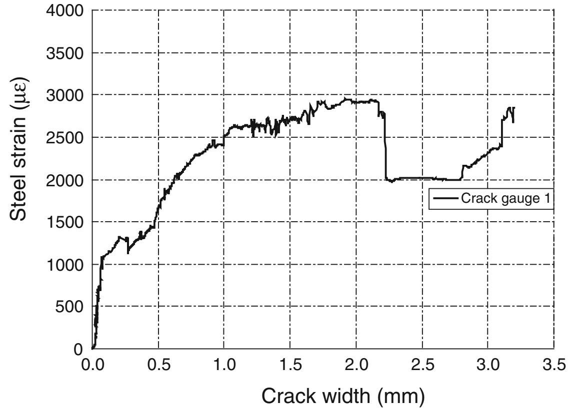

Fig. 8 Crack width expansion versus steel strain for HS1 ($h = 250$ mm)

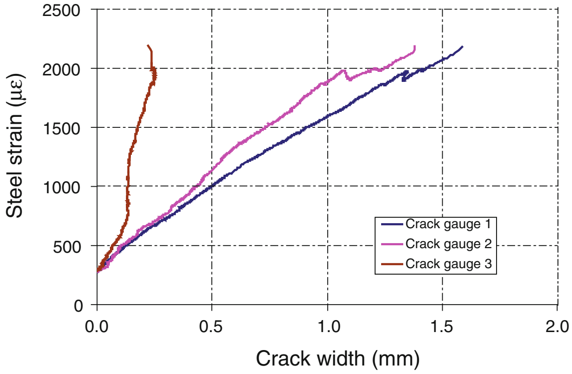

Fig. 9 Crack width expansion versus steel strain for NS2 ($h = 300$ mm)

crack width can be influenced by as much as 28% when the concrete cover increases from 60 to 70 mm for the same bar spacing. This is compared to 0%

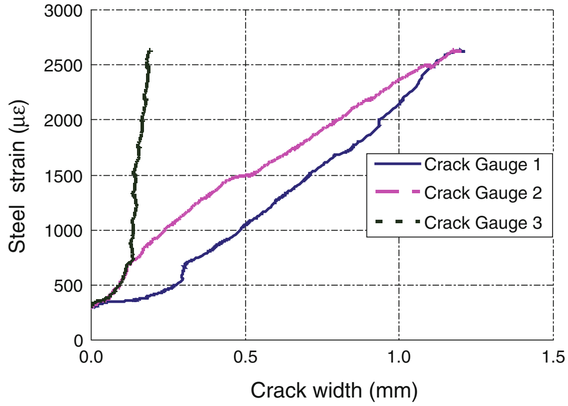

Fig. 10 Crack width expansion versus steel strain for HS2 ($h = 300$ mm)

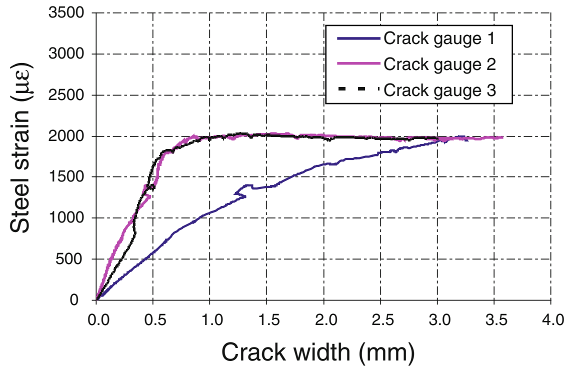

Fig. 11 Crack width expansion versus steel strain for HS3 ($h = 300$ mm)

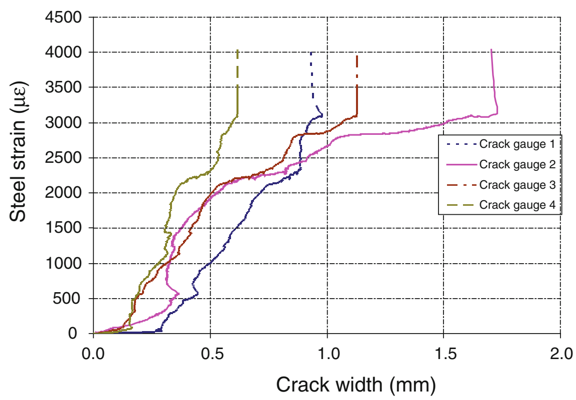

Fig. 12 Crack width expansion versus steel strain for HS4 ($h = 350$ mm)

increase estimated by ACI 318-08 [11] and EC2 (2004) [15], 3% decrease calculated by CSA-S474-04 [12] and NS 3474 E (1989) [13] and 22% increase

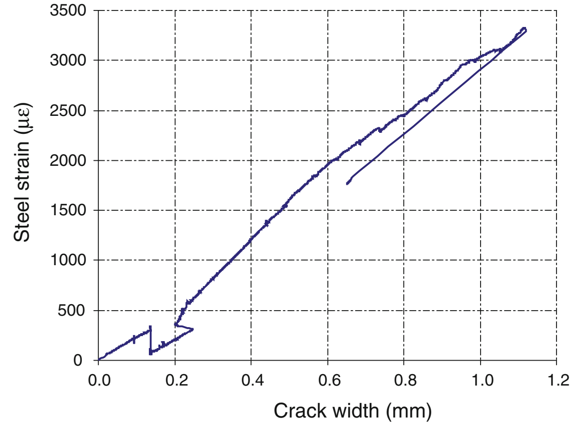

Fig. 13 Crack width expansion versus steel strain for HS5 ($h = 350$ mm)

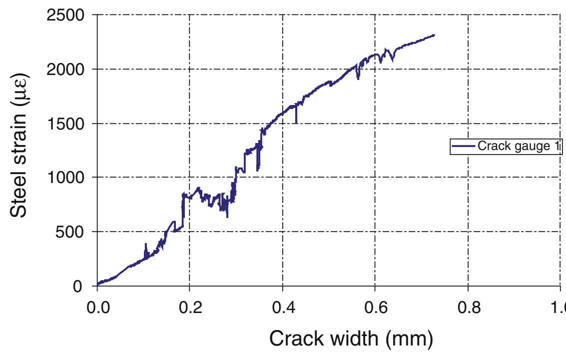

Fig. 14 Crack width expansion versus steel strain for NS3 ($h = 400$ mm)

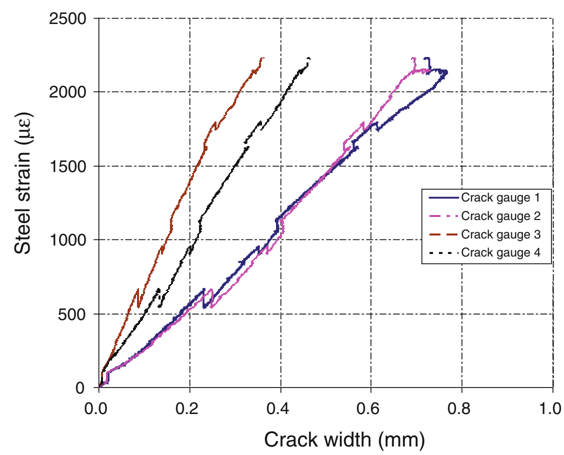

Fig. 15 Crack width expansion versus steel strain for HS6 ($h = 400$ mm)

Table 2 Comparison between the calculated crack width values using code formulae with the measured experimental values

Group no.	Slab no.[a]	Experiment S_m (mm)	Experiment w_k (mm)	Proposed eq. w_k (mm)	ACI w_c (mm)	CSA w_m (mm)	NS w_m (mm)	CEB-FIP w_k (mm)	EC2 w_k (mm)
I	NS1	245	0.465	0.724	0.470	0.638	0.649	0.413	0.661
	HS1	263	0.402	0.775	0.470	0.634	0.649	0.294	0.661
	NS2	261	0.607	0.705	0.470	0.619	0.630	0.493	0.663
	HS2	246	0.596	0.767	0.470	0.615	0.630	0.415	0.663
	HS3	247	0.590	0.935	0.470	0.689	0.705	0.326	0.745
II	HS4	221	0.581	0.927	0.470	0.663	0.679	0.431	0.740
	HS5	264	0.435	0.835	0.370	0.514	0.526	0.376	0.605
	NS3	250	0.439	0.733	0.278	0.471	0.480	0.366	0.587
	HS6	210	0.469	0.852	0.278	0.469	0.480	0.344	0.587

[a] *NS* normal strength slabs, *HS* high strength slabs

calculated using CEB-FIP (1990) [14] model code. This means that for the same bar spacing, increasing the concrete cover by about 17% resulted in increasing the crack width by about 28%. Test results by Hossin and Marzouk [10] revealed that as the concrete cover was increased by 67% (from 30 mm to 50 mm), the average crack width increased by 90% experimentally. Results by Hossin and Marzouk [10] were based on slabs with a total thickness of 150–200 mm. The conclusions that relate the crack width to the concrete cover should address the member depth (height of effective embedment thickness, h_{ef}). In the case of the experimental work conducted by Hossin and Marzouk [10], the crack width was very sensitive to the concrete cover depth due to the relatively thick concrete covers used compared to the slabs small depths.

Two test specimens HS2 and HS3 were identical except reinforcement ratio. Both slabs had the same bar spacing, the same concrete cover but with different bar diameters. Slab HS2 had a reinforcement ratio equal to 0.73% with a bar diameter of 25 mm and was designed using ACI 318-08 [11] requirements for minimum flexural reinforcement while slab HS3 had a reinforcement ratio equal to 0.43% with a bar diameter of 20 mm and was designed using equation proposed by Rizk and Marzouk [17]. The test results indicated that the effect of changing the bar diameter was negligible. It should be noted also that both specimens had the same average crack spacing.

Two specimens of Group II (HS4 and HS5) were designed and specifically tested to determine the effect of increasing bar spacing on crack width while keeping concrete cover constant. It can be seen, in general, that the maximum crack width is increased as the bar spacing is increased. In addition, it appears that the effect of increasing the bar spacing on the crack width is much profound than the effect of increasing the concrete cover.

The data of Group II showed that for the range of bar spacing tested, the maximum crack width can be influenced by as much as 50% when the bar spacing was increased from 217 mm to 368 mm. This means that for the same concrete cover increasing the bar spacing by about 70% resulted in increasing the crack width by about 50%.

As the first group (Group I) was designed to investigate the effect of pure flexure failure on crack properties. A comparison of the experimental results of the average crack width measurements of the two tested Groups indicated that the mode of failure had no effect on the size of the crack width.

All codes neglect the effect of concrete strength on crack width. The CEB-FIP (1990) [14] model code is the only code that takes into account the effect of concrete strength when calculating crack width. Test results of Group I indicated that increasing the concrete strength from 35 MPa to 70 MPa resulted in about 10–15% decrease in crack width.

Group II included four thick specimens with the same 70 mm thick concrete cover. Test results revealed that crack control can still be achieved by limiting the spacing of the reinforcing steel despite using thick concrete cover.

6 Analytical investigation

The proposed model is based on estimating the crack spacing first, followed by determining the steel strain at the serviceability limit from cross section analysis. Finally the tension stiffening contribution is considered. In this research the presented crack width model is based on a proposed crack spacing model by Rizk and Marzouk [1]. As shown in Fig. 16a, stretching bars in direction X with the concrete surrounding the bars will result in another crack at a distance $= S_{\mathrm{mx}}$. A sufficient bond force is developed at this location that is just large enough to induce a maximum tensile stress equal to the tensile strength of concrete. As a result of the two-way action of the slabs, stretching the bars in a perpendicular direction results in splitting circumferential forces in direction X. Another crack at a distance $= S_{\mathrm{mx}}$ may form when it is over the length of S_{mx}, a sufficient bond force is developed, which together with the splitting stresses along the transverse bars, is just large enough to induce a maximum tensile stress equal to the tensile strength of concrete.

The presented theoretical model for calculating crack width for two-way slabs combines the known effect of bond stress with the splitting bond stress in the transverse direction, which is due to the action of two-way slabs. The bond stress can be assumed as a parabolic variation with a peak stress that occurs at the mid section between the two cracks. This assumption can greatly simplify the mathematical formulation in calculating the bond stress. The resulting parabolic bond stress distribution between two successive flexural cracks is shown in Fig. 16b.

The crack spacing formed in direction X, can be estimated as follows:

$$S_{\mathrm{mx}} = \frac{k_t f_{\mathrm{ctm}} A_{\mathrm{ctx}} - 0.67\, d_{\mathrm{by}} f_{\mathrm{ctm}}}{\frac{2}{3}\pi\, d_{\mathrm{bx}} f_{\mathrm{bo}}\, n_x} \tag{12}$$

The constant k_t accounts for the distribution of tensile stress in section 1-1 (Fig. 16) on the effective

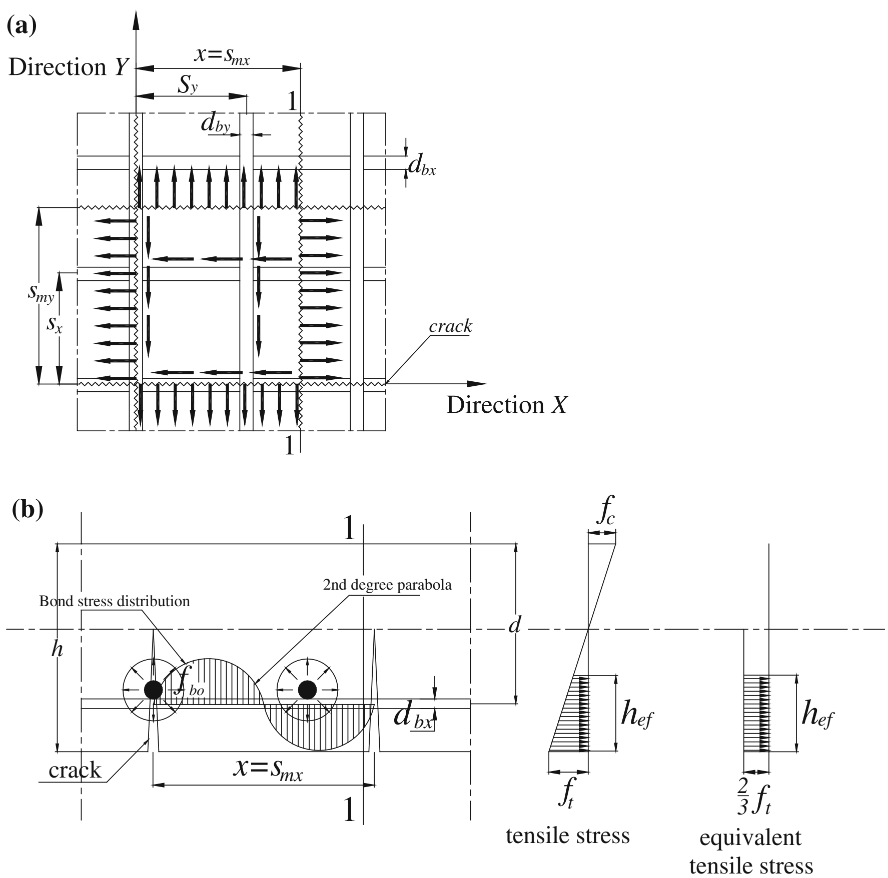

Fig. 16 Distribution of bond stress, splitting stress and tensile stress over a section: (**a**) A plan of a two-way plate; (**b**) Cross section of two-way plate

area of concrete A_{ctx}, f_{ctm} is the mean tensile strength value of the concrete that is calculated according to the CEB-FIP (1990) [14] model code and f_{bo} is the peak bond stress calculated using Eqs. 16, 17 or 23. Similarly, the spacing of cracks formed in direction Y, can be estimated as follows:

$$S_{my} = \frac{k_t f_{ctm} A_{cty} - 0.67\, d_{bx} f_{ctm}}{\frac{2}{3}\pi\, d_{by} f_{bo}\, n_y} \tag{13}$$

Equations 12 and 13 give the crack spacing in directions X and Y respectively at a given stage of loading. In order to use the above expression, values of k_t, A_{ctx}, A_{cty}, f_{ctm} and f_{bo} must be estimated. The constant k_t is a tensile stress factor that depends on the distribution of tensile stress on concrete areas A_{ctx} and A_{cty}. In the proposed expression, k_t can be taken as equal to unity for plates and two-way slabs having concrete covers of ($C_c < 2.5\ d_b$). For plates and two-way slabs with thick concrete covers that are greater than 2.5 d_b and less than 5.0 d_b, k_t can be taken as equal to 0.67. The values of A_{ctx} and A_{cty}, which are the effective stretched area of concrete in the X and Y direction, are assumed to be:

$$A_{ctx} = h_{efx}\, b \tag{14}$$

$$A_{cty} = h_{efy}\, b \tag{15}$$

where h_{ef} is the effective embedment thickness (shown in Fig. 1). The constant k_t accounts for the distribution of tensile stress in Sect. 1-1 on the effective area of concrete, A_{ctx}. The number of bars per unit width in X direction is n_x.

The value of the peak bond strength, f_{bo}, is calculated using the CEB-FIP (1990) [14] Model Code equation. The CEB-FIP (1990) [14] Model Code (Table 3.1.1) provides the following expression for calculating peak bond stress for confined and unconfined concrete for different bond conditions:

$$f_{bo} = \mu\sqrt{f_c'}(\text{MPa}) \tag{16}$$

For cases where failure is initiated by splitting of the concrete (unconfined concrete), the coefficient μ is taken equal to unity and hence f_{bo} at the serviceability limit is calculated as follows:

$$f_{bo} = 1.0\sqrt{f_c'}(\text{MPa}) \tag{17}$$

It should be noted that Eq. 17 is only valid for concrete covers equal or less than 2.5 d_b ($C_c \le 2.5\ d_b$), C_c is the clear concrete cover, for plates and two-way slabs with thick concrete covers greater than the radius of the effective embedment zone ($C_c > 2.5\ d_b$), it was found that a value of 0.75 for the coefficient μ will be more consistent, so Eq. 17 can be modified as follows:

$$f_{bo} = 0.75\sqrt{f_c'}(\text{MPa}) \tag{18}$$

This is due to the fact that such plates act as cross sections that contain two separate materials, a reinforced concrete part and a plain concrete part.

6.1 Maximum crack width

The two important factors which determine the width of the crack are the crack spacing and the steel strain; both of these depend on the external loading on the slab. Crack spacing decreases with increasing load and stabilizes after reinforcement reaches a critical stress. Further stress increases act only to widen existing cracks. The cracks that form at the stage of cracking moment are farthest apart, at this stage the spacing of cracks is the maximum crack spacing, S_{max}. With increasing the load, more cracks are developed. When steel stress reaches a critical value, crack spacing stabilizes. Increasing the load acts only to widen the existing cracks.

Crack width at the level of reinforcement is determined as the relative difference in elastic extensions of steel and surrounding concrete, both extensions are measured with respect to the zero-slip point. The extension of steel at the cracked section ε_s is evaluated as follows:

$$\varepsilon_s = \frac{f_s}{E_s} \tag{19}$$

The corresponding contraction of concrete ε_c at the cracked section is determined as follows:

$$\varepsilon_c = \frac{2\pi f_{bo} S_m}{9 E_c h_{ef}} \tag{20}$$

where E_c is concrete modulus of elasticity. The average crack width at the extreme tension surface can be calculated as follows:

$$w_m = S_m\, \xi\, \varepsilon_{sm} \tag{21a}$$

$$w_m = S_m\, \xi\left(\varepsilon_s \frac{h_2}{h_1} - \varepsilon_c\right) \tag{21b}$$

where S_m is the average crack spacing (stabilized crack stage) obtained from Eqs. 12 or 13, ξ is a dimensionless coefficient between 0 and 1, representing the effect of the participation of concrete in the tension zone to stiffness of the member [EC2 (2004)] [15], ε_{sm} is the average strain in steel at the stage at which the crack width is determined, h_1 is the distance from centroid of the tension steel to the neutral axis and h_2 is the distance from extreme tension fiber to the neutral axis. This follows from an assumption of linear variation of strain.

The tension stiffening contribution is estimated without consideration for the steel reinforcement ratio, size of the concrete cover and concrete member thickness. A tension stiffening model based on fracture mechanics concepts and tension properties of high-strength concrete was developed by Marzouk and Chen [18]. The model can account for the concrete mix design properties and the steel reinforcement contribution through two sets of constants.

The ratio between maximum crack width $w_{\max}$ and average crack width w_m had been suggested by Rizkalla and Hwang [19] to be equal to 1.55. CEB-FIP (1990) [14] recommended a value of 1.70 for flexural members. The maximum crack width at the extreme tension fiber is obtained from:

$$w_{\max} = 1.55\, w_m \tag{22}$$

6.2 Crack width for beams and one-way slabs

The proposed equation can be used to calculate the crack width for beams and one-way slabs by modifying the peak bond strength f_{bo}, according to the CEB-FIP (1990) [14] Model Code provisions (clause 3.1.1). For cases where failure is initiated by shearing of the concrete between rebars ribs, f_{bo} is calculated as follows:

$$f_{bo} = 1.25\sqrt{f_c'}\ (\text{MPa}) \tag{23}$$

The crack spacing can be estimated as follows:

$$S_m = \frac{k_t f_{ct} A_{ct}}{\frac{2}{3}\pi\, d_b f_{bo}\, n} \tag{24}$$

where n is the number of bars per unit width. The constant k_t is a tensile stress factor that depends on the distribution of tensile stress on concrete area A_{ct}. In the proposed expression, k_t can be taken as equal to 0.67 for beams and one-way slabs. The average and maximum crack width can be calculated using Eqs. 21 and 24.

7 Proposed model versus different code predictions

In order to verify the validity of the proposed crack control model, the model was applied to predict the average crack width of normal weight concrete test slabs reported in the literature. The results indicate that there exists a very good correlation between theoretical and measured maximum crack width values and between theoretical and calculated maximum crack width values using different codes' formulae. In this paper, the model has been applied to thirty tests, to predict the characteristic crack width of beams, one-way and two-way concrete slabs. The geometry of test slabs can be found in references 7, 8 and 10, analysis and the results are shown in Tables 3, 4, 5 and include twelve test results of Gilbert and Nejadi [9], ten test results of Frosch et al. [8] with different concrete covers and different bar spacing, eight test results of Hossin and Marzouk [10] with different concrete strengths, different concrete covers and different bar spacing.

It is also worth emphasizing that the slabs analyzed cover many variables that influence crack width such as concrete strength, bar spacing and concrete cover. Bearing this in mind as well as the fact that the tests themselves are one-to-one scale models as far as the slab thickness of the prototype and the inevitable scatter of test results in concrete behavior, the theoretical model developed here is an excellent representation of the physical behavior of test specimens.

8 Summary and conclusions

The experimental and theoretical results can be summarized as follows:

- The test results of Group I show that as the concrete cover increases, the maximum crack width increases. The data showed that the maximum crack width can be influenced by as much as 28% when the concrete cover was increased from 60 to 70 mm for the same bar spacing.
- The data of Group II showed that the maximum crack width can be influenced by as much as 50% when the bar spacing was increased from 217 mm to 368 mm, this means that for the same concrete

Table 3 Comparison between the calculated crack width values using codes' formulae with the measured experimental values for test specimens by Gilbert and Nejadi [9]

Slab no.[a]	f'_c (MPa)	Bar spacing (mm)	Concrete cover C_c (mm)	ACI w_c (mm)	CSA w_m (mm)	NS w_m (mm)	CEB-FIP w_k (mm)	EC2 w_k (mm)	Experiment w_k (mm)	Proposed eq. w_k(mm)
B1-a	36	150	40	0.192	0.365	0.372	0.381	0.460	0.330	0.496
B1-b	36	150	40	0.192	0.365	0.372	0.381	0.460	0.380	0.496
B2-a	36	180	25	0.230	0.313	0.318	0.381	0.390	0.300	0.452
B2-b	36	180	25	0.230	0.313	0.318	0.381	0.390	0.430	0.452
B3-a	36	90	25	0.116	0.228	0.231	0.290	0.311	0.200	0.312
B3-b	36	90	25	0.116	0.228	0.231	0.290	0.311	0.200	0.312
S1-a	36	308	25	0.393	0.367	0.373	0.319	0.366	0.330	0.445
S1-b	36	308	25	0.393	0.367	0.373	0.319	0.366	0.280	0.445
S2-a	36	154	25	0.197	0.256	0.260	0.255	0.292	0.250	0.322
S2-b	36	154	25	0.197	0.256	0.260	0.255	0.292	0.250	0.322
S3-a	36	103	25	0.132	0.210	0.214	0.207	0.255	0.180	0.251
S3-b	36	103	25	0.132	0.210	0.214	0.207	0.255	0.230	0.251

[a] *B* beam, *S* slab

Table 4 Comparison between the calculated crack width values using codes' formulae with the measured experimental values for test specimens by Frosch et al. [8]

Slab no.[a]	f'_c (MPa)	Bar spacing (mm)	Concrete cover C_c (mm)	ACI w_k (mm)	CSA w_m (mm)	NS w_m (mm)	CEB-FIP w_k (mm)	EC2 w_k (mm)	Experiment w_k (mm)	Proposed eq. w_k (mm)
B-6	46.6	152	38	0.229	0.368	0.373	0.330	0.369	0.381	0.355
B-9	44.4	229	38	0.343	0.469	0.477	0.430	0.446	0.483	0.505
B-12	44.5	305	38	0.456	0.571	0.580	0.487	0.524	0.457	0.618
B-18	47.4	457	38	0.684	0.773	0.786	0.473	0.679	0.381	0.744
E12-6	46.7	152	38	0.249	0.401	0.406	0.367	0.369	0.406	0.354
E12-9	46.4	229	38	0.373	0.511	0.519	0.485	0.446	0.635	0.497
E12-12	45.7	305	38	0.497	0.622	0.631	0.561	0.524	0.584	0.612
E12-18	46.8	457	38	0.745	0.843	0.855	0.583	0.679	0.787	0.746
E6-9	46.1	229	38	0.373	0.511	0.519	0.485	0.446	0.457	0.498
E18-9	46.0	229	38	0.373	0.511	0.519	0.485	0.446	0.584	0.499

[a] *B* black bars, *E* epoxy coated bars

cover increasing the bar spacing by about 70% results in increasing the crack width by about 50%.

- Test results of Group II revealed that crack control can still be achieved by limiting the spacing of the reinforcing steel despite using thick concrete cover.
- The ACI 318-08 [11] expression does not account for concrete cover effect on crack width for concrete structure members with the same bar spacing.
- The analytical investigation revealed that the crack widths calculated using CSA-S474-04 [12] and NS 3473 E (1989) [13] were relatively close.
- Crack control can be achieved by limiting bar spacing. The proposed model in Eqs. 12, 13 or 24 allows designers to specify bar spacing during the design process to control flexural crack width to an acceptable limit.

Table 5 Comparison between the calculated crack width values using codes' formulae with the measured experimental values for test specimens by Hossin and Marzouk [10]

Slab no.[a]	f_c' (MPa)	Bar spacing (mm)	Concrete cover C_c (mm)	ACI w_k (mm)	CSA w_m (mm)	NS w_m (mm)	CEB-FIP w_k (mm)	EC2 w_k (mm)	Experiment w_k (mm)	Proposed eq. w_k (mm)
NSC1	35.0	150	30	0.192	0.335	0.341	0.439	0.436	0.406	0.355
HSC1	68.5	150	50	0.192	0.408	0.419	0.350	0.501	0.772	0.569
HSC2	70.0	150	60	0.193	0.446	0.458	0.333	0.533	0.950	0.763
HSC3	66.7	200	30	0.256	0.402	0.412	0.428	0.508	0.486	0.382
HSC4	61.2	250	30	0.319	0.476	0.488	0.472	0.586	0.483	0.383
HSC5	70.0	100	30	0.129	0.199	0.204	0.137	0.246	0.327	0.343
NSC2	33.0	240	30	0.307	0.377	0.383	0.393	0.425	0.248	0.292
NSC3	34.0	240	40	0.307	0.332	0.338	0.207	0.325	–	0.672

[a] *NSC* normal strength slabs, *HSC* high strength slabs

Acknowledgments The authors are grateful to the Natural Sciences and Engineering Research Council of Canada (NSERC) for providing the funds for the project. Sincere thanks are due to Mr. Matthew Curtis, Mr. Shawn Organ, Mr. Darryl Pike and the Technical Staff of the Structural Engineering Laboratory of Memorial University of Newfoundland for their assistance during the preparation of the specimens and during testing. Sincere thanks are extended to Capital Ready Mix Ltd., Newfoundland, for providing the concrete for this project.

References

1. Rizk E, Marzouk H (2010) A new formula to calculate crack spacing for concrete plates. ACI Struct J 107(1):43–52
2. Makhlouf H, Malhas F (1996) The effect of thick concrete cover on the maximum flexural crack width under service load. ACI Struct J 93(3):257–265
3. ACI Committee 318 (1989) Building code requirements for reinforced concrete (ACI 318-89). American Concrete Institute, Detroit
4. BSI (1985) Structural use of concrete: Code of Practice for Special Circumstances, BS 8110-85: Part 1 and 2: British Standard Institution, London
5. Frosch R (1999) Another look at cracking and crack control in reinforced concrete. ACI Struct J 96(3):437–442
6. Gergely P, Lutz L (1968) Maximum crack width in reinforced concrete flexural members, causes, mechanism, and control of cracking concrete. SP-20, American Concrete Institute, pp 87–117
7. ACI Committee 318 (1995) Building code requirements for structural concrete (ACI 318-95) and Commentary (ACI 318M-95), ACI 318-95, American Concrete Institute. Farmington Hills, Michigan
8. Frosch R, Blackman D, Radabaugh R (2003) Investigation of bridge deck cracking in various bridge superstructure systems, FHWA/IN/JTRP Report No. C-36-56YY, File No. 7-4-50, School of Civil Engineering, Purdue University, West Lafayette
9. Gilbert R, Nejadi S (2004) An experimental study of flexural cracking in reinforced concrete members under sustained loads, UNICIV Report No. R-435, School of Civil and Environmental Engineering, University of New South Wales, Sydney, Australia
10. Hossin M, Marzouk H (2009) Crack width estimation for concrete plates. ACI Struct J 107(3):282–290
11. ACI Committee 318 (2008) Building code requirements for structural concrete (ACI 318-08) and Commentary (ACI 318M-08), ACI 318-08. American Concrete Institute, Farmington Hills
12. Canadian Standards Association (CSA) (2004) Concrete structures. CSA-S474-04, Mississauga, Ontario, Canada
13. Norwegian Standard, NS 3473 E (1989) (English Translation), Concrete structures, design rules, Norwegian council for building standardization. Oslo, Norway
14. Comité Euro-International Du Béton-Fédération de la Précontrainte (CEB-FIP), Model Code 1990, Bulletin D'Information, No. 203–305, Lausanne, Switzerland
15. Eurocode 2 (EC2) (2004) Design of concrete structures-Part 1-1: General rules and rules for buildings, 2004-1-1
16. Marzouk H, Hussein A (1991) Experimental investigation on the behavior of high-strength concrete slabs. ACI Struct J 88(6):701–713
17. Rizk E, Marzouk H (2009) New formula to calculate minimum flexure reinforcement for thick high-strength concrete plates. ACI Struct J 106(5):656–666
18. Marzouk H, Chen Z (1993) Nonlinear analysis of normal and high-strength concrete slabs. Can J Civil Eng 20(4):696–707
19. Rizkalla S, Hwang L (1984) Crack prediction for members in uniaxial tension. ACI Struct J 81(6):572–579